

CHAPTER 161

PROTECTION OF MARITIME STRUCTURES AGAINST SHIP COLLISIONS

by

Kazuki Oda* and Shoshichiro Nagai**

ABSTRACT

This paper deals with the analytical and experimental studies on a new device to prevent the accidents of ship collisions with maritime structures. The practical protection device was designed on the basis of this study and it has been in use for the prevention of ship collisions of a class of 1,000 G/T with a boring tower for the geological survey of the sea beds of a narrow straits in which quite a many ships navigate.

INTRODUCTION

For the recent several years, maritime structures such as drilling platforms, intake towers of cooling water for thermal and/or nuclear power plants and also bridge piers have been constructed nearshore and offshore throughout the world. When they are constructed in seas or straits where many ships navigate, there exists a great possibility of ship collisions with such maritime structures.

In the case of Japan in which several long bridges are being constructed to span the narrow straits with strong tidal currents and quite a many navigation ships, this problem has been considered to be very serious from the points of view of safety navigation as well as the protection of the bridge pier from ship collisions. Even during the terms of the preliminary geological survey of the sea beds at the projected construction sites of the piers of the long bridges, there have been already a lot of accidents of ship contacts with the boring towers for the geological survey. Therefore, it has been urgently needed to find ways for prevention of the accidents of contacts and collisions with erection jackets during the construction of the piers and the piers themselves after the completion of the bridges.

As a result, a new protection device capable of turing securely the original course of approaching vessels to the piers in front of them was proposed by our laboratory and the Honshu-Shikoku Bridge Authority. It consists of three large buoys anchored to the sea bottom and two pressure pneumatic rubber tubes-lines which are tightened with the restoring forces of mooring buoy system and float on the water surface as shown in Fig.1.

* Assistant Professor of Hydraulic Engineering, Faculty of Engineering, Osaka City University, Osaka, Japan.

** Professor of Hydraulic Engineering, Faculty of Engineering, Osaka City University, Osaka, Japan.

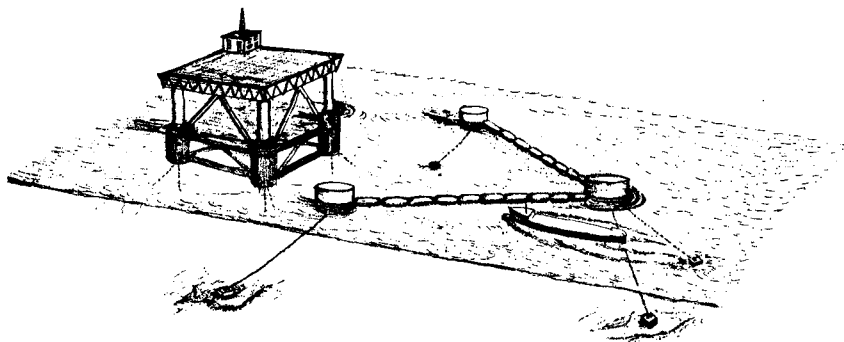


Fig.1. Schematic diagram of the protection device

The analytical and experimental studies were carried out in the hydraulics laboratory of Osaka City University to examine the effect of the proposed protection device and to predict the tensions of the mooring lines of the buoys and the rubber tubes-lines.

APPROACHING CONDITIONS OF SHIPS TO THE DEVICE

(1) Gross tonnages of ships

The results of the investigation on ships passing through the Akashi Straits, the Eastern Bisan Straits and the Kurushima Straits in the Seto Inland Sea, which was conducted by Kobe Mercantile Marine College and Maritime Safety Agency of Japan in July of 1971, are shown in Figs.2, 3 and 4 respectively.

According to these figures, the average number of ships per day passed through is more than 1,000 in every straits. Especially in the Akashi Straits, it comes up to more than 2,000. It will be noted, however, that more than 80% of total ships, including almost all of passenger boats, ferry boats and fishing boats, are smaller ships than 500 G/T while large ships greater than 3,000 G/T are very few in every straits.

It is considered to be quite difficult to protect the piers from the collisions of ships greater than 10,000 to 20,000 G/T by the aid of the device proposed here because of their much larger momentum. For the protection of piers against the collisions of such larger ships, the another way using a steel jacket fender system fixed on the pier is being examined now.

Consequently, it was decided that the gross tonnages of ships considered here to be approaching vessels were 1,000 to 2,000 G/T.

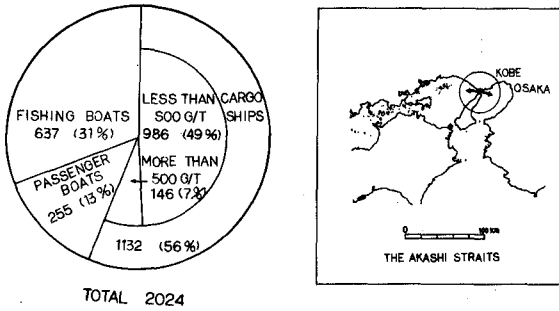


Fig.2. Statistics of ships per day passed through the Akashi Straits

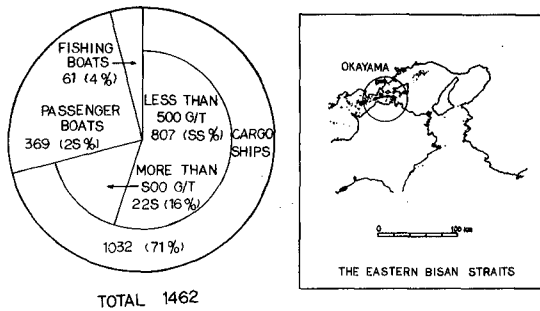


Fig.3. Statistics of ships per day passed through the Eastern Bisan Straits

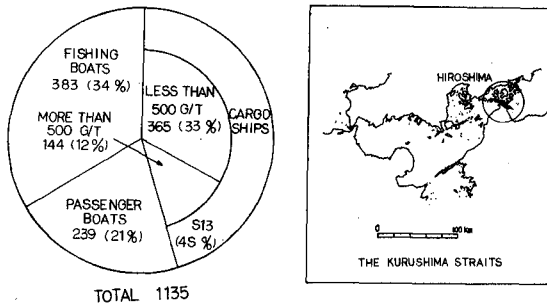


Fig.4. Statistics of ships per day passed through the Kurushima Straits

(2) Approaching speeds and heading angles

According to an annual report "Statistics of Vessels in 1970" published by Ministry of Transportation, 83 to 87% of vessels between 1,000 to 3,000 G/T travel with a speed of 10 to 14 knots.

Since the traveling speeds of ships, however, will be decelerated by the captain in emergency, it may be considered that the approaching speeds into the protection device are less than the usual traveling speeds. As a result, the approaching speeds of ships of a class of 1,000 to 2,000 G/T into the protection device were decided to be 8 to 10 knots in this study.

In general, ships are steered to be almost paralleled to the seaways regulated in narrow straits. Accordingly, the approaching heading angles into the device were taken to be 10 to 15 degrees to the direction of seaway.

THEORETICAL ANALYSIS

1. Basic equations of motion of a ship

A set of co-ordinate axes, x_G, y_G with the origin fixed at the center of gravity of a ship as shown in Fig.5 is used to set up basic equations of motion of a ship. The x_G - and y_G - axes represent the longitudinal and transverse horizontal axes of the ship respectively.

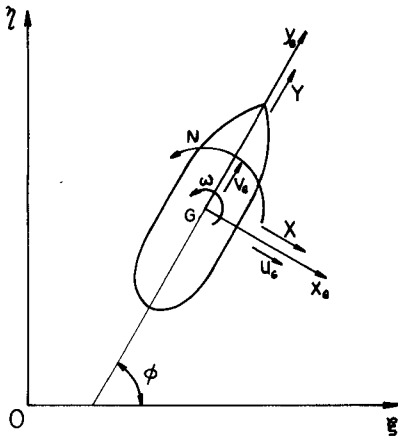


Fig.5. Co-ordinate system

By reference to these co-ordinate axes, equations of motion of the ship in horizontal plane can be written as follows.

$$\left. \begin{aligned} m(\dot{u}_G - \omega v_G) &= X && \text{(sway)} \\ m(\dot{v}_G + \omega u_G) &= Y && \text{(surge)} \\ I_{ZZ}\dot{\omega} &= N && \text{(yaw)} \end{aligned} \right\} (1)$$

where: m = mass of the ship

I_{ZZ} = moment of inertia about the vertical axis through the center of gravity of the ship

u_G, \dot{u}_G = components of the ship velocity and acceleration in x_G -axis direction

v_G, \dot{v}_G = components of the ship velocity and acceleration in y_G -direction

$\omega, \dot{\omega}$ = angular velocity and acceleration about the vertical axis
 X, Y and N = total external forces and moments including hydrodynamic and other non-hydrodynamic forces and moments

The effects of waves and winds are not considered in this treatment. The effects of the coupling roll, pitch, and heave motions into horizontal motion are assumed negligibly small.

The components of external forces X, Y and moments N are expressed as follows for the case of zero rudder angle in linear theory:

$$\left. \begin{aligned} X &= X_u u_G + X_{\dot{u}} \dot{u}_G + X_v v_G + X_{\dot{v}} \dot{v}_G + X_{\omega} \omega + X_{\dot{\omega}} \dot{\omega} + f_x \\ Y &= Y_u u_G + Y_{\dot{u}} \dot{u}_G + Y_v v_G + Y_{\dot{v}} \dot{v}_G + Y_{\omega} \omega + Y_{\dot{\omega}} \dot{\omega} + f_p + f_y \\ N &= N_u u_G + N_{\dot{u}} \dot{u}_G + N_v v_G + N_{\dot{v}} \dot{v}_G + N_{\omega} \omega + N_{\dot{\omega}} \dot{\omega} + f_{\phi} \end{aligned} \right\} \quad (2)$$

where f_x, f_y and f_{ϕ} are the components of non-hydrodynamic external forces and moments. f_p is propulsive forces. $X_{\dot{u}}, X_{\dot{v}}, X_{\dot{\omega}}, Y_{\dot{u}}, Y_{\dot{v}}, Y_{\dot{\omega}}$, and $N_{\dot{u}}, N_{\dot{v}}, N_{\dot{\omega}}$ are hydrodynamic coefficients concerning added masses. $X_u, X_v, X_{\omega}, Y_u, Y_v, Y_{\omega}$ and N_u, N_v, N_{ω} are hydrodynamic coefficients concerning damping forces.

On the assumption that the ship is symmetric with respect to the longitudinal and transverse centerline plane, and that the center of gravity of added mass is coincident with that of the ship, $X_v, X_{\dot{v}}, X_{\dot{\omega}}, Y_u, Y_{\dot{u}}, Y_{\dot{\omega}}, N_{\dot{u}}$ and $N_{\dot{v}}$ can be regarded as zero.

Furthermore, neglecting the effect of damping forces and moments except the damping term $Y_v v_G$ in the surge motion and using nonlinear damping forces $C v_G^2$ instead of linear damping forces $Y_v v_G$, Eq.(2) may be simplified as follows.

$$\left. \begin{aligned} X &= -m_x \dot{u}_G + f_x \\ Y &= -m_y \dot{v}_G - C v_G^2 + f_p + f_y \\ N &= -J_{ZZ} \dot{\omega} + f_{\phi} \end{aligned} \right\} \quad (3)$$

where: $-m_x = X_{\dot{u}}$ added mass in X_G -axis direction
 $-m_y = Y_{\dot{v}}$ added mass in Y_G -axis direction
 $-J_{ZZ} = N_{\dot{\omega}}$ added moment of inertia about the vertical axis
 $C =$ dimensional coefficient of total ship resistances

2. Equations of motion of the ship after contact with the protection device

(1) Co-ordinate system

The co-ordinate system and the symbols used in the theoretical analysis concerning the protection device are shown in Fig.6.

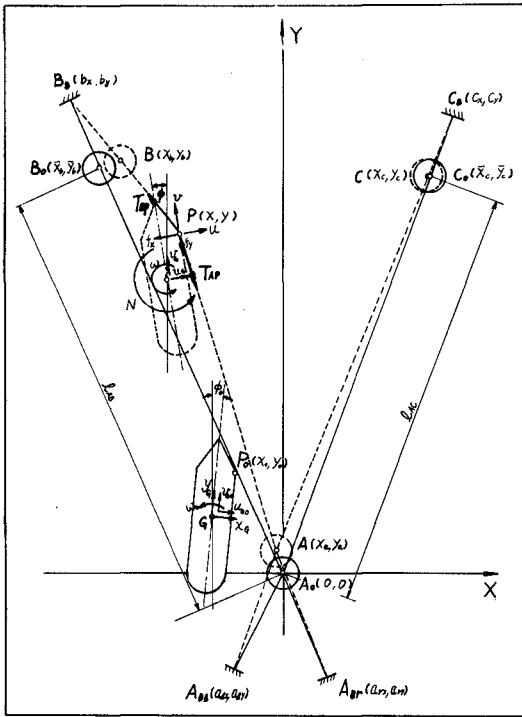


Fig.6. Co-ordinate system and definition sketch of the protection device

The definitions of the symbols in Fig.6 are as follows.

X, Y = co-ordinate axes fixed on the earth with the origin at the center of the main buoy

x_G, y_G = co-ordinate axes with the origin at the center of gravity of the ship

A_{B1}, A_{Br}, B, C = anchor points of each buoy

l_{AB}, l_{AC} = initial distances between the main buoy and the sub-buoy

A, B, C = center points of each buoy

p = contact point with the rubber tubes-line

u_G, v_G = components of the ship velocity in the directions of x_G - and y_G -axes at the center of gravity G

u, v = components of the ship velocity in the directions of x_G - and y_G -axes at the contact point p

ω = angular velocity about the vertical axis of the ship

ϕ = heading angle of the ship to the Y-axis

f_x, f_y = components of the reaction forces on the contact point exerted by the deflection of the rubber tubes-line

The subscript 0, herein, denotes the quantities at the initial time.

(2) Basic assumptions

The following assumptions are introduced to simplify the theoretical analysis on the protection device.

- (a) The movements of the main buoy A are negligibly small.
- (b) Therefore, the movements of the rubber tubes-line AC of the opposite side to the line AB contacting with the ship can be also neglected.
- (c) The configurations of the mooring lines of every buoy can be regarded as straight without any slack.
- (d) The elongations of the mooring lines of the buoys and the rubber tubes-line can be neglected.
- (e) The hydrodynamic forces induced by the movement of the sub-buoy and the rubber tubes-line may be neglected.
- (f) The frictional forces between the rubber tubes-line and the ship hull are minor.
- (g) While the ship is in contact with the rubber tubes-line, the propulsive forces of the ship is constant and the rudder angles is stationarily zero.
- (h) The point of the ship in contact with the rubber tubes-line is stationarily on the bow shoulder of the ship.

(3) External forces and moments on the ship

On the above assumptions, the external forces and moments acting on the ship in contact with the rubber tubes-line are obtained as follows.

Referring to Fig. 7, components of the reaction forces, f_x and f_y on the contact point exerted by the deflection of the rubber tubes-line from the original straight line can be expressed as follows.

$$\left. \begin{aligned} f_x &= - \{ T_{BP} \sin(\theta_{BP} - \phi) - T_{AP} \sin(\theta_{AP} - \phi) \} \\ f_y &= - \{ T_{AP} \cos(\theta_{AP} - \phi) - T_{BP} \cos(\theta_{BP} - \phi) \} \end{aligned} \right\} \quad (4)$$

where: T_{AP}, T_{BP} = tensions of the segments AP and BP of the rubber tubes-line respectively

θ_{AP}, θ_{BP} = angles between the segments AP, BP of the rubber tubes-line and Y-axis respectively

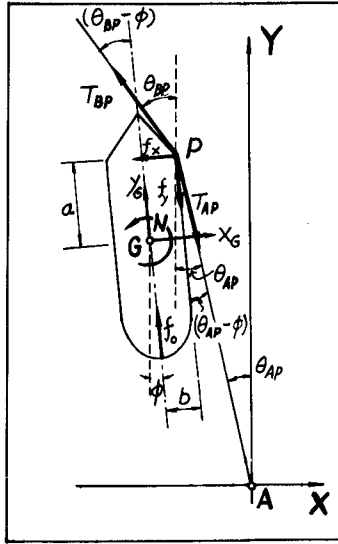


Fig.7. Definition sketch of the external forces and moments

Since the assumption (f) yields $T_{AP} = T_{BP}$, Eq.(4) can be rewritten as follows.

$$\left. \begin{aligned} f_x &= -T_{AB} \{ (\sin\theta_{BP} - \sin\theta_{AP}) \cos\phi - (\cos\theta_{BP} - \cos\theta_{AP}) \sin\phi \} \\ f_y &= -T_{AB} \{ (\cos\theta_{AP} - \cos\theta_{BP}) \cos\phi + (\sin\theta_{AP} - \sin\theta_{BP}) \sin\phi \} \end{aligned} \right\} \quad (5)$$

where T_{AB} , which is used in place of T_{AP} and T_{BP} , is the tensions of the rubber tubes-line.

From the geometrical relations shown in Fig.8, the following equations are derived.

$$\left. \begin{aligned} \sin\theta_{AP} &= -\frac{x}{\sqrt{x^2 + y^2}} \\ \cos\theta_{AP} &= \frac{x}{\sqrt{x^2 + y^2}} \\ \sin\theta_{BP} &= \frac{x - b_x}{\sqrt{(x - b_x)^2 + (y - b_y)^2}} \\ \cos\theta_{BP} &= -\frac{y - b_y}{\sqrt{(x - b_x)^2 + (y - b_y)^2}} \end{aligned} \right\} \quad (6)$$

Substituting Eq.(6) into (5), Eq.(7) is obtained.

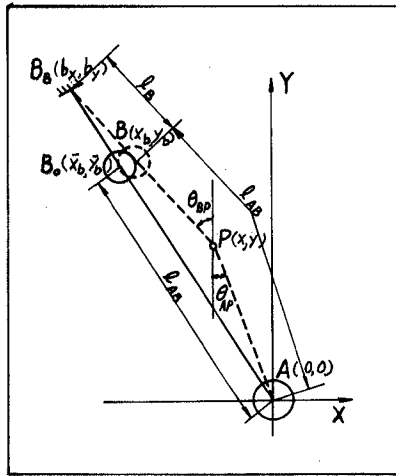


Fig.8. Geometrical relations of the rubber tubes-line

$$\left. \begin{aligned}
 f_x &= -T_{AB} \left\{ \left(\frac{x - b_x}{\sqrt{(x - b_x)^2 + (y - b_y)^2}} + \frac{x}{\sqrt{x^2 + y^2}} \right) \cos\phi \right. \\
 &\quad \left. + \left(\frac{y - b_y}{\sqrt{(x - b_x)^2 + (y - b_y)^2}} + \frac{y}{\sqrt{x^2 + y^2}} \right) \sin\phi \right\} \\
 f_y &= -T_{AB} \left\{ \left(\frac{y - b_y}{\sqrt{(x - b_x)^2 + (y - b_y)^2}} + \frac{y}{\sqrt{x^2 + y^2}} \right) \cos\phi \right. \\
 &\quad \left. + \left(\frac{x - b_x}{\sqrt{(x - b_x)^2 + (y - b_y)^2}} + \frac{x}{\sqrt{x^2 + y^2}} \right) \sin\phi \right\}
 \end{aligned} \right\} \quad (7)$$

External moments f_ϕ around the vertical axis through the center of gravity of the ship induced by these forces f_x, f_y are given by Eq.(8).

$$f_\phi = - (af_x - bf_y) \quad (8)$$

where a and b are the lengths of moment arms of f_x and f_y around the center of gravity of the ship shown in Fig.7 respectively. According to the assumption (h), these lengths are considered to be constant while the ship contacts with the line.

On the other hand, from the equations of equilibrium of the forces acting on the point B and the geometrical relations shown in Fig.9, the tensions T_{AB} of the rubber tubes-line in Eq.(7) can be written as follows.

$$T_{AB} = \{w_0 A_B (h_B - \sqrt{S_B^2 - l_B^2}) - W_B\} \frac{l_B}{\sqrt{S_B^2 - l_B^2}} \quad (9)$$

where: w_0 = specific weight of water

A_B = area of waterplane of the sub-buoy

W_B = weight of the sub-buoy

S_B = length of the mooring line of the sub-buoy

l_B = horizontal distance between the sub-buoy and its anchor point given by Eq.(10)

$$l_B = \sqrt{x^2 + y^2} + \sqrt{(x - b_x)^2 + (y - b_y)^2} - l_{AB} \quad (10)$$

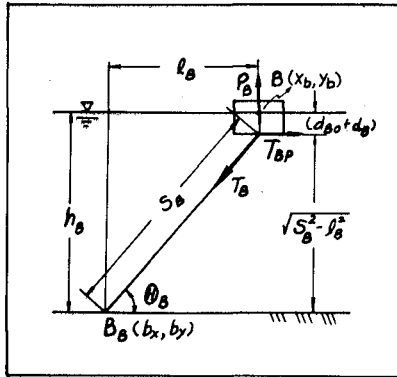


Fig.9. Definition sketch of the forces on the sub-buoy

(4) Total ship resistances and propulsive forces

In general, total ship resistances R_T consisting of frictional resistances and residual resistances which include wave making resistances and eddy resistances are given by Eq.(11).

$$R_T = C v_G^2 \quad (11)$$

where: v_G = velocity of a ship in the direction of the longitudinal axis

C = dimensional coefficient of total ship resistances expressed by Eq. (12)

$$C = (C_f + C_r) \frac{1}{2} \rho S$$

where: ρ = density of water

S = area of wetted surface of the ship hull

C_f = coefficient of frictional resistances

C_r = coefficient of residual resistances

Assuming that a ship approaches into the protection device with a constant speed, the propulsive forces can be considered to equal to the total resistances of the ship traveling with the constant approaching velocity v_G in the direction of the longitudinal axis. Thus, the propulsive forces of the ship can be written as follows.

$$f_p = C v_G^2 \quad (13)$$

where f_p is the propulsive forces.

(5) Tensions of the mooring lines of the buoys

From the equations of equilibrium of the forces acting on the point A and the geometrical relations shown in Fig.10, the tensions of two mooring lines of the main buoy are given by the following equations respectively.

$$\begin{aligned} T_{Ar} &= \sec \theta_{A0} \operatorname{cosec} 2\alpha_0 \{ T_{AB} \sin(\alpha_0 - \theta_{Ap}) + (T_{AC})_0 \sin(\alpha_0 - \beta_0) \} \\ T_{Al} &= \sec \theta_{A0} \operatorname{cosec} 2\alpha_0 \{ T_{AB} \sin(\alpha_0 - \theta_{Ap}) - (T_{AC})_0 \sin(\alpha_0 + \beta_0) \} \end{aligned} \quad (14)$$

where: T_{Ar} , T_{Al} = tensions of the mooring lines AA_r and AA_l respectively

T_{AB} = tensions of the rubber tubes-line AB

$(T_{AC})_0$ = initial tensions of the rubber tubes-line AC

θ_{A0} = initial vertical angle of inclination of the mooring line of the main buoy

$2\alpha_0$, $2\beta_0$ = initial horizontal angle between the two mooring lines of the main buoy and initial angle between the two rubber tubes-lines respectively

In the same way, by references to Fig.9 again, the tensions of the mooring line of the sub-buoy are obtained as follows.

$$T_B = \{ w_0 A_B (h_B - \sqrt{S_B^2 - l_B^2}) - W_B \} \frac{S_B}{\sqrt{S_B^2 - l_B^2}} \quad (15)$$

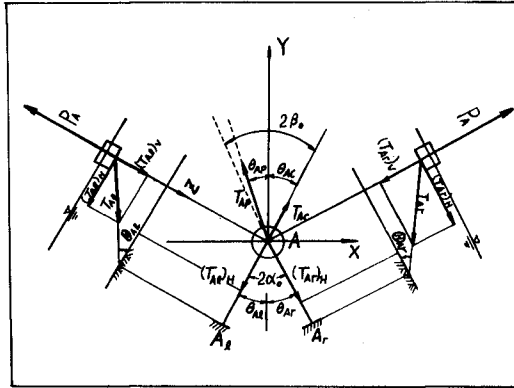


Fig.10. Definition sketch of the forces on the main buoy

(6) Equations of motion of the ship

Substituting Eq.(3) into Eq.(1), equations of motion of the ship after contact with the rubber tubes-line of the protection device can be expressed as follows.

$$\left. \begin{aligned} (m + m_x) \dot{u}_G &= m\omega v_G + f_x \\ (m + m_y) \dot{v}_G &= -m\omega u_G - C v_G^2 + f_p + f_y \\ (I_{ZZ} + J_{ZZ}) \dot{\omega} &= f_\phi \end{aligned} \right\} \quad (16)$$

Using the velocity components u and v of the point of the ship in contact with the rubber tubes-line in the directions of X- and Y-axes fixed on the earth as shown in Fig.11, the velocity components u_G and v_G of the center of gravity of the ship in x_G - and y_G -axes directions can be denoted as follows.

$$\left. \begin{aligned} u_G &= u \cos\phi + v \sin\phi + a\omega \\ v_G &= v \cos\phi - u \sin\phi - b\omega \end{aligned} \right\} \quad (17)$$

Substituting Eq.(17) into Eq.(16), the final equations of motion of the ship after contact with the rubber tubes-line can be written as follows.

$$\left. \begin{aligned} \dot{x} &= u, \quad \dot{y} = v, \quad \dot{\phi} = \omega \\ u &= -\left\{ \frac{\cos\phi}{M_x} + \frac{a}{I_Z} (a \cos\phi + b \sin\phi) \right\} f_x \end{aligned} \right\}$$

(to be continued to the next page)

$$\begin{aligned}
 & + \left\{ \frac{\sin\phi}{M_y} + \frac{b}{I_z} (a \cos\phi + b \sin\phi) \right\} f_y \\
 & - \frac{\sin\phi}{M_y} \{ f_p - C(v \cos\phi - u \sin\phi - b\omega)^2 - \omega v \\
 & + m\omega \left\{ \frac{\cos\phi}{M_x} (v \cos\phi - u \sin\phi - b\omega) + \frac{\sin\phi}{M_y} (u \cos\phi + v \sin\phi + a\omega) \right\} \\
 & \dot{v} = \left\{ \frac{\sin\phi}{M_x} + \frac{a}{I_z} (a \sin\phi - b \cos\phi) \right\} f_x \\
 & + \left\{ \frac{\cos\phi}{M_y} - \frac{b}{I_z} (a \sin\phi - b \cos\phi) \right\} f_y \\
 & + \frac{\cos\phi}{M_y} \{ f_p - C(v \cos\phi - u \sin\phi - b\omega)^2 + \omega u \\
 & + m\omega \left\{ \frac{\sin\phi}{M_x} (v \cos\phi - u \sin\phi - b\omega) - \frac{\cos\phi}{M_y} (u \cos\phi + v \sin\phi + a\omega) \right\}
 \end{aligned} \tag{18}$$

where: $M_x = m + m_x$, $M_y = m + m_y$, $I_z = I_{zz} + J_{zz}$

Eq.(18) is six simultaneous non-linear differential equations and can be solved by means of numerical analysis using the Runge-Kutta-Gill method.

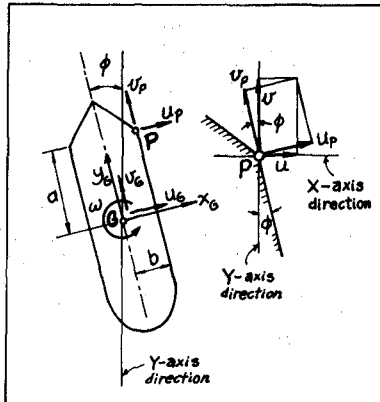


Fig.11. Definition sketch of the velocities

MODEL EXPERIMENTS

Model experiments were conducted on a 1 to 50 model scale in the wave basin which is 42 m long, 12 m wide and 0.75 m deep as shown in Fig.12. A radio-controlled model ship corresponding to 880 G/T cargo ship in prototype was used in the experiments.



Fig.12. Wave basin used in the experiments

The arrangement and dimension of the model of the protection device are shown in Fig.13.

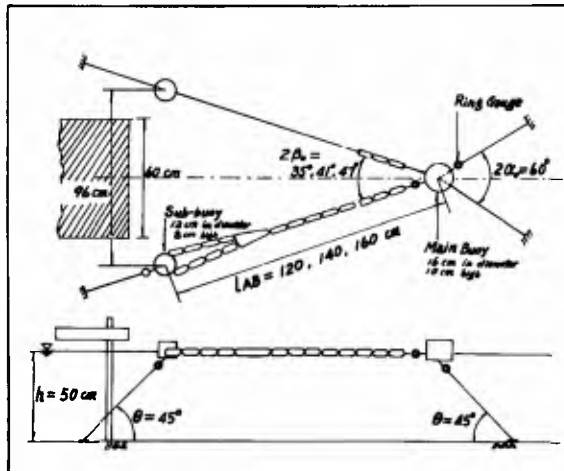


Fig.13. Arrangement and dimension of the model of the protection device

The variable quantities measured in the experiments are the approaching speeds v_{G_0} and the heading angles ϕ_0 of the model ship to the rubber tubes-line, the distances p_0 between the center A of the main buoy and the initial contact point P_0 , the lateral displacements δ_B of the sub-buoy in the X-axis direction, the tensions T_{Ar} , T_B of the mooring lines of the main buoy and the sub-buoy and the tensions T_{AB} of the rubber tubes-line as shown in Fig. 14.

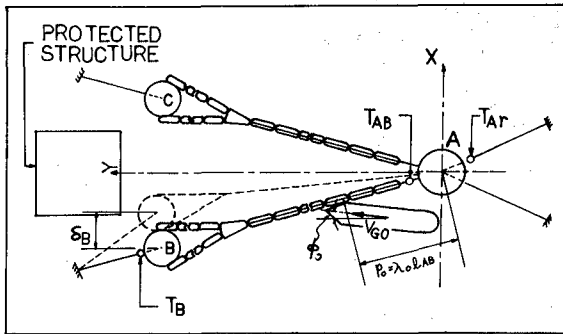


Fig.14. Variable quantities measured in the experiments

The tensions were measured with sensitive ring-gauges made of brass which straingauges are mounted on both sides. Custom-made mini-turnbuckles were used to facilitate the adjustment of the initial tensions of the rubber tubes-lines.

The horizontal motions of the ship and the displacements of the sub-buoy were measured by analyzing 16 mm movies taken from a tower 6 m high above the water level. Fig.15 shows an example of frame-photographs of the 16 mm movies. Fig.16 shows the model ship approaching to the rubber tubes-line and going forward contacting with the line.

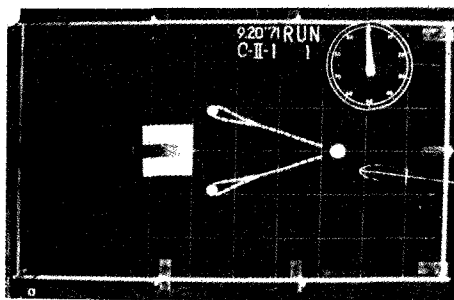


Fig.15. A frame-photograph of 16 mm movies

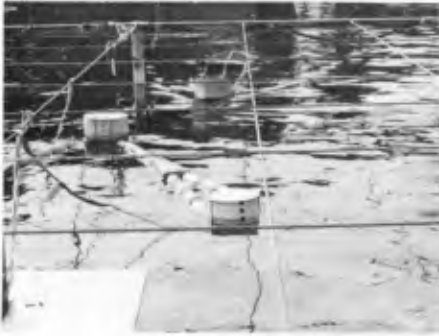


Fig.16(a). The model ship approaching to the rubber tubes-line



Fig.16(b). The model ship going forward contacting with the line

COMPARISON BETWEEN THEORY AND EXPERIMENTS

The theoretical values obtained by means of numerical analysis of the maximum tensions $(T_{AB})_{max}$ of the rubber tubes-line, the maximum tensions $(T_{Ar})_{max}$, $(T_B)_{max}$ of the main buoy and sub-buoy, and the maximum lateral displacements $(\delta_B)_{max}$ of the sub-buoy, were compared with the experimental ones as shown in Figs.17, 18, 19 and 20 respectively.

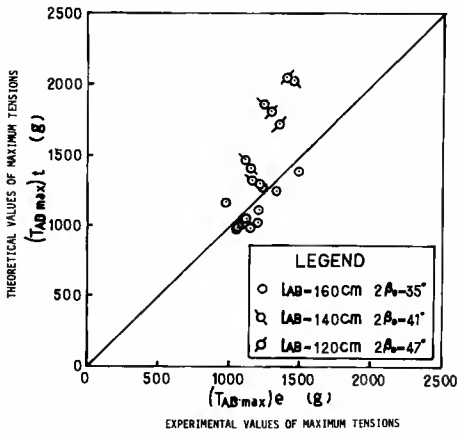


Fig.17. Comparison between the theoretical and experimental values on $(T_{AB})_{max}$

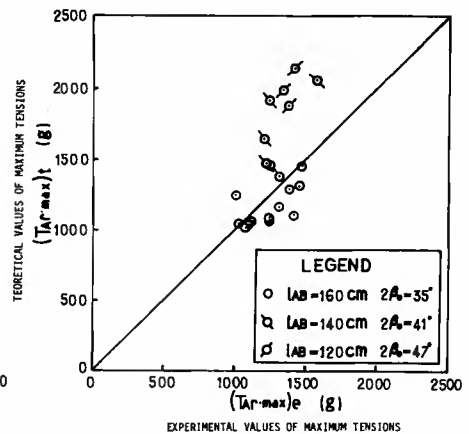


Fig.18. Comparison between the theoretical and experimental values on $(T_{Ar})_{max}$

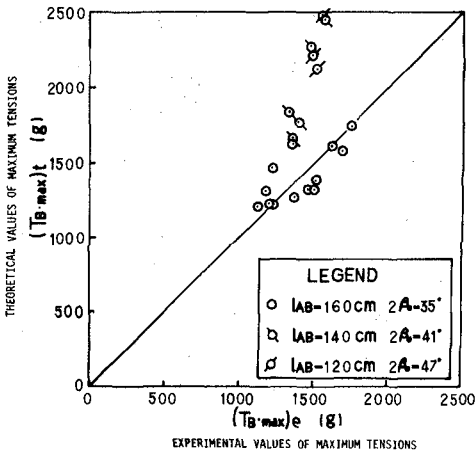


Fig. 19. Comparison between the theoretical and experimental values on $(T_B)_{\max}$

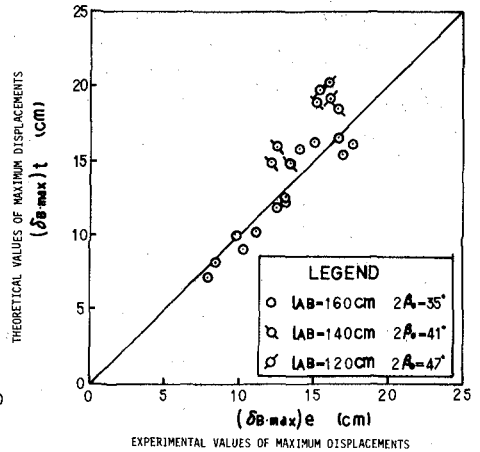


Fig. 20. Comparison between the theoretical and experimental values on $(\delta_B)_{\max}$

These figures show that the agreement between the theoretical and experimental values concerning $(T_{AB})_{\max}$, $(T_{Ar})_{\max}$, $(T_B)_{\max}$ and $(\delta_B)_{\max}$ is good for the case of $l_{AB} = 160$ m, $2\beta_0 = 37^\circ$ but poor for the case of $l_{AB} = 140$ m, $2\beta_0 = 41^\circ$ and $l_{AB} = 120$ m, $2\beta_0 = 47^\circ$.

Namely, it may be said that the theoretical values reasonably agree with the experimental ones for the case of longer distances between the main buoy and the sub-buoy and smaller angles between the rubber tubes-lines, however, the theoretical values much deviate from the experimental results for the case of shorter distances and larger angles.

The major reasons for the much deviation may be considered as the followings.

In general, since the heading angles of the ship relative to the rubber tubes-line are larger in the case of larger angle between the two tubes-lines, the ship contacts with the rubber tubes-line near the bow end in such cases. In addition, in the case of shorter distances between the main buoy and the sub-buoy, the lateral motions of the sub-buoy and the rubber tubes-line tend to be quicker than in the case of longer distances. Therefore, it may be considered that the assumptions (e) and (h) are no longer reasonable for such cases.

From the comparison between the theoretical and experimental results, it may be concluded that the theory is limited to its application for the case of $l_{AB}/L_{pp} \geq 1.3$, $\psi_0 \leq 25^\circ$. Herein, L_{pp} is the length between perpendiculars of the ship and ψ_0 is the initial heading angle relative to the rubber tubes-line.

APPLICATION FOR PRACTICAL USE

A practical protection device for prevention of ship collisions of a class of 1,000 G/T against the floating drilling platform with the deck 43 m by 43 m shown in Fig.21, was designed under the following practical conditions;

gross tonnage of the approaching ship:	1,000 G/T
distance between the main buoy and sub-buoy:	$l_{AB} = 100 \text{ m}$
angle between two rubber tubes-lines:	$2\beta_0 = 36.5^\circ$
horizontal angle between two mooring chains of the main buoy:	$2\alpha_0 = 36.5^\circ$
vertical angles of the mooring chains:	$\theta_0 = 45^\circ$
area of water plane of the sub-buoy:	$A_B = 40 \text{ m}^2$
water depth (effects of the tidal range were taken into consideration):	$h = 50 \pm 1.0 \text{ m}$
approaching speed of the ship:	$v_{G0} = 10 \text{ kt}$
initial heading angle of the ship:	$\phi_0 = 0^\circ$
nondimensional initial contact position ($\lambda_0 = p_0/l_{AB}$):	$\lambda_0 = 0.5$
initial tensions of the rubber tubes-line at Mean Water Level:	$(T_{AB})_0 = 50 \text{ t}$



Fig.21. Picture of the floating drilling platform

The essential results of the numerical calculations for the practical device are summarized in Table 1.

Table 1. Essential Results of the Numerical Calculations for the Practical Device

Essential quantities	At Low Water Level	At High Water Level
Initial values		
$(T_{AB})_0$ (t)	21.2	88.3
$(T_B)_0$ (t)	30.0	125
$(T_{AR})_0$ (t)	21.2	88.3
Maximum values		
$(T_{AB})_{max}$ (t)	157	186
$(T_B)_{max}$ (t)	210	253
$(T_{AR})_{max}$ (t)	179	221
$(\delta_B)_{max}$ (m)	12.9	10.8

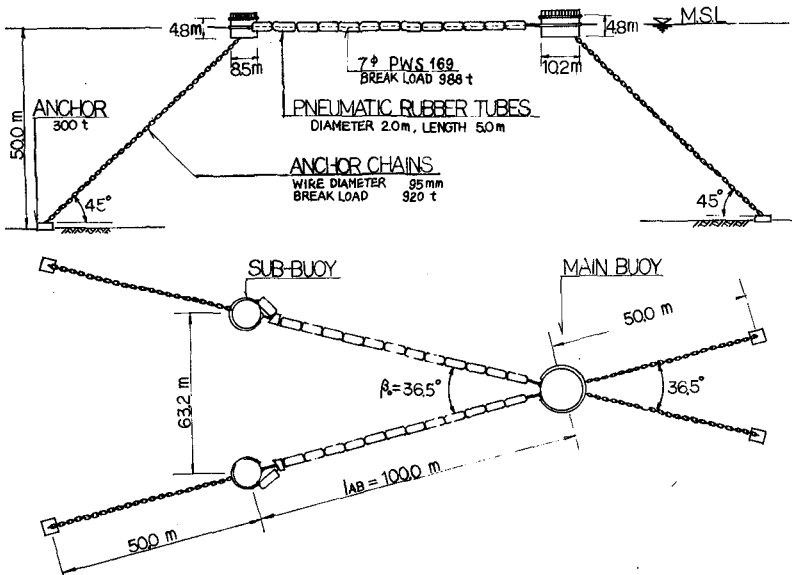


Fig.22. Schematic diagram of the practical protection device

Fig.22 shows the schematic diagram of the practical protection device designed on the basis of the above results of the numerical calculations.

The rubber tubes-line is composed of fourteen pressure pneumatic rubber tubes each 2 m in diameter and 5 m long with a steel pipe along the central axis and a parallel wire rope 105 mm in diameter with a break load of 988 t.

The main buoy is 10.2 m in diameter and 4.8 m high and the sub-buoy 8.5 m in diameter and 4.8 m high.

Anchor chains 95 mm in wire diameter with a break load of 920 t are used for the mooring line of the main-buoy and sub-buoy, and specially moulded cast iron sinkers 300 t in weight in the air were used for the anchors of the buoys.

The initial tensions of the rubber tubes-line can be arbitrarily adjusted by changing the buoy draft by means of pulling up the mooring chains into the buoy using an oil pressure jack equipped on the buoy deck.

Fig.23 shows the practical protection device set in front of the floating drilling platform in the Akashi Straits.



Fig.23. Picture of the practical protection device

CONCLUSION

The new device to protect maritime structures from ship collisions proposed here was proved in experimental and theoretical ways to be very useful to prevent the collisions of ships up to 1,000 to 2,000 G/T with usual traveling speeds of 10 to 14 knots.

The tensions of the rubber tubes-line and the mooring lines of the main buoy and sub-buoy, and the lateral displacements of the sub-buoy can be completely predicted by solving the equations of motion of the ships after contact with the rubber tubes-line by means of numerical calculations using the Runge-Kutta-Gill method.